THE JOURNAL OF BIOLOGICAL CHEMISTRY VOL. 287, NO. 20, pp. 16681–16688, May 11, 2012

Hairless Plays a Role in Formation of Inner Root Sheath via Regulation of *Dlx3* Gene*[S]

Received for publication, November 4, 2011, and in revised form, February 27, 2012 Published, JBC Papers in Press, March 22, 2012, DOI 10.1074/jbc.M111.320770

Bong-Kyu Kim[‡], Hwa-Young Lee[‡], Jee-Hyun Choi[‡], Jeong-Ki Kim[‡], Jong-Bok Yoon[§], and Sungjoo Kim Yoon[‡1]

From the [‡]Department of Medical Life Sciences, The Catholic University of Korea, Seoul, 137-701, Korea and [§]Department of Biochemistry and Translational Research Center for Protein Function Control, Yonsei University, Seoul 120-749, Korea

Background: HR is a transcriptional factor that regulates hair cycle and hair follicle development.
Results: Decreased expression of *Dlx3* by HR down-regulates expression of IRS keratins.
Conclusion: HR plays a role in formation of IRS through regulation of *Dlx3*, consequently, IRS keratin expression.
Significance: These data provide an explanation for abnormal formation of IRS in Hr^{Hp}/Hr^{Hp} skin and suggest a role of HR in IRS formation.

The *Hairless* (*Hr*), a transcription factor, is expressed in the suprabasal cell layer of the interfollicular epidermis and the lower portion of the hair follicle epithelium, where its expression is dependent on the hair cycle. Recently, we reported a new *Hr* mutant mouse, Hr^{Hp}, in which the hairless protein (HR) was overexpressed. In this study, we documented abnormal formation of inner root sheath (IRS), suppressed expression of *Dlx3*, and IRS keratins in the Hr^{Hp}/Hr^{Hp} skin. We also found that HR down-regulated *Dlx3* mRNA expression through suppression of *Dlx3* promoter activity. In addition, we showed that Dlx3 regulated the expression of IRS keratins. Our results demonstrate that regulation of *Dlx3* by HR affects the IRS keratin expression, thus modulating the formation of IRS of hair follicle.

In mammals, the hair follicle (HF)[2] is the unique mini organ of the skin that produces hair and is composed of functionally different epithelial layers, such as the outer root sheath, inner root sheath (IRS), and hair shaft (1). HF is unique in that continuous cycling consisting of growth (anagen), regression (catagen), and rest (telogen) stages is required to produce and maintain hairy phenotype (2, 3). Many genes take part in the regulation of formation and cycling of HFs (4).

One of these genes, *hairless* (*Hr*), is mainly detected in the HFs and the suprabasal layers of the interfollicular epidermis (5, 6). *Hr* encodes a 130-kDa protein (HR), which plays an important role in HF regeneration (7). HR acts as a transcriptional co-repressor through binding to nuclear receptors, such as the vitamin D receptor, thyroid hormone receptor, and retinoic acid-like orphan receptor α (8–10). Many *Hr* mutant mice have been reported and studied to understand the function of *Hr* (11–15). Recently, we reported the *Hr* mutant mice called "Hairpoor" (Hr^{Hp}), whose genome harbors a T-to-A substitution at position 403 in the non-coding exon 2 of *Hr* (16). Differently from other *Hr* mutations with loss of function of *Hr*, this mutation causes overexpression of HR through translational derepression (17, 18). Hr^{Hp} heterozygous mice show partial hair loss at an early age and progress to complete alopecia. This phenotype resembles that of the human hair disorder called Marie Unna hereditary hypotrichosis (OMIM-146550), which is caused by similar mutations in the 5′ UTR of the *HR* gene. Interestingly, Hr^{Hp} homozygous mice show total alopecia (16, 17).

The Distal-less 3 (*Dlx3*) is a mouse homolog of *Drosophila Distal-less* homeodomain protein that belongs to the members of the Dlx vertebrate family (19). Dlx3 acts as a transcriptional activator and plays a critical role in the development of epidermis, bone, and placenta (20–23). Mutations of *Dlx3* were found to be responsible for the defects in teeth and bone development called the Tricho-Dento-Osseous syndrome (24, 25). In HF, *Dlx3* is expressed widely in the hair shaft, hair matrix, and IRS (26, 27). Previously, the selective ablation of *Dlx3* was shown to cause complete alopecia, due to failure of formation of the hair shaft and IRS (24, 27).

In this study, we investigated the Hr^{Hp}/Hr^{Hp} skin to define the consequence of overexpressed HR in HF structure. We found that the expression of *Dlx3* and IRS keratins was down-regulated in Hr^{Hp}/Hr^{Hp} skin. And we showed that *Dlx3* expression was suppressed by HR, thus mediating subsequent regulation of keratin expression in IRS using *in vitro* system. Our results show that HR plays an important role in IRS formation via regulation of *Dlx3* expression, which explains abnormal formation of IRS in Hr^{Hp}/Hr^{Hp} skin.

EXPERIMENTAL PROCEDURES

Mice—Hr^{Hp} mice were maintained as described previously (28). All animal experiments were approved by the Institutional Animal Care and Use Committee of the Catholic University of Korea. All experiments were carried out in accordance with the guidelines for animal experimentation.

* This work was supported by the Basic Science Research Program of the National Research Foundation of Korea; the Ministry of Education, Science and Technology Grant 2009-0066830 (to S.-j. K. Y.); and the Korea Research Foundation Grant KRF-2006-005-J04502, funded by the Korean Government.
[S] This article contains supplemental Table 1 and Figs. 1–4.
[1] To whom correspondence should be addressed. Tel.: 82-2-2258-7476; Fax: 82-2-594-2385; E-mail: sjkyoon@catholic.ac.kr.
[2] The abbreviations used are: HF, hair follicle; IRS, inner root sheath; Hr, Hairless; Dlx3, Distal-less 3; Hr^{Hp}, Hairpoor; Krt, Keratin; Tchh, trichohyalin; P7, postnatal day 7; VDR, vitamin D receptor.

Scanning Electron Microscopy (SEM) and Transmission electron microscopy (TEM)—Wild-type and Hr^{Hp}/Hr^{Hp} skin samples at postnatal day 7 (P7) and P14 were fixed in 2% glutaraldehyde and 0.5% paraformaldehyde in 0.1 M sodium cacodylate buffer containing 0.1 M sucrose and 3 mM $CaCl_2$. Fixed samples were post-fixed in 1% osmium tetroxide in 0.1 M sodium phosphate and dehydrated in ethanol. Skin samples were either sputtered with gold and examined using JSM LV 5410 (Jeol) or embedded and visualized using JEM1010 (Jeol).

RT-PCR and Real Time PCR—Total RNA was extracted from the skins of wild-type and Hr^{Hp}/Hr^{Hp} mice and PAM212 cells using TRIzol reagent (Invitrogen) according to the manufacturer's instructions. Single-stranded cDNAs were synthesized using the PrimeScript 1st strand cDNA synthesis kit (Takara). PCR and real time PCR were performed using Peltier Thermal Cycler-100 (MJ Research) and Mx3000P (Stratagene) as described previously (29). Each primer sequence and cycling condition was listed in supplemental Table 1. All transfection experiments were normalized against transfection efficiency determined by β-galactosidase activity. Relative expression level was normalized against glyceraldehyde-3-phosphate dehydrogenase (GAPDH) gene expression.

Western Blot Analysis—Protein extracts were prepared from wild-type and Hr^{Hp}/Hr^{Hp} mouse skin or PAM212 cells using radioimmune precipitation assay buffer (150 mM sodium chloride, 1% Nonidet P-40, 0.5% sodium deoxycholate, 0.1% SDS, 50 mM Tris-HCl, pH 8.0) according to the standard method. Protein was quantified using the Bradford method using BSA as control. Three hundred micrograms (mouse skin) or 200 μg of protein (cells) were used for Western blot analysis as described previously (29). Rabbit polyclonal HR (Abfrontier) and Dlx3 (Santa Cruz Biotechnology) antibodies and mouse polyclonal β-actin antibody (Applied Biological Materials, Richmond, CA) were used for Western blot at a dilution of 1: 2500, 1:1000, and 1:5000, respectively. The protein signals were visualized using the ECL system (Amersham Biosciences).

In Situ Hybridization—The back skin sections of the wild-type and Hr^{Hp}/Hr^{Hp} mice were dehydrated in EtOH and fixed in 4% paraformaldehyde and then treated with 0.25% acetic anhydride in 0.1 M Tris. Prehybridization was performed in a solution of 50% formamide and 5× sodium chloride and sodium citrate solution (SSC) at 55 °C for 30 min, and then the sections were incubated in hybridization solution (50% formamaide, 5× SSC, 5 μg/ml heparin, 500 μg/ml yeast tRNA, 1 mM EDTA, and 0.1% CHAPS) containing 1 μg of digoxigenin-labeled *Dlx3* probe overnight at 60 °C. After washing and blocking, the sections were incubated with anti-digoxigenin antibody conjugated with alkaline phosphatase (Roche Applied Science) overnight at 4 °C, and then the signals visualized using nitro blue tetrazolium/5-bromo-4-chloro-3-indolyl phosphate substrates (Promega).

Immunohistochemistry—Immunohistochemistry was performed as described previously (17). Dlx3 antibody (Santa Cruz Biotechnology, 1:500) and Alexa Fluor 546 goat anti-rabbit secondary antibody (Invitrogen, 1:500) were used. Fluorescence signal was observed with a fluorescent microscope (Olympus).

Plasmid Construction—DNA fragments containing putative *Dlx3* promoter region (−1608 to −1 bp, −1608 to −1031 bp, −1064 to −577 bp, and −593 to −1 bp) or the full-length *Dlx3* cDNA or vitamin D receptor (VDR) cDNA were amplified by PCR using the Expand High Fidelity enzyme (Roche Applied Science) from the genomic DNA or skin cDNAs of the wild-type mice, respectively. Forward and reverse primer sequences of *Dlx3* are listed in supplemental Table 1. These PCR products were subcloned into either pcDNA 3.1 (Invitrogen) or pGLuc-vector DNA (Invitrogen). For the *Dlx3* probe, *Dlx3* cDNA (843–1444 bp; NM_010055) was amplified using PCR and subcloned into pGEMT-easy (Promega). After linearization of the plasmids with SmaI, the probe was prepared using DIG-labeling kit (Roche Applied Science) following the manufacturer's instructions.

Cell Culture and Transient Transfection Experiment—PAM212 cell line (mouse keratinocyte cells) was maintained in DMEM (Invitrogen) containing 10% FBS with 5% CO_2 at 37 °C incubator. *Hr* full-length cDNA construct was described previously (29). Transfection experiments were performed using polyethyleneimine (Sigma-Aldrich) according to the manufacturer's instructions. Cells (8×10^5/dish) were seeded in 60-mm dishes in triplicate, and 1 to 3 μg of either *Hr* cDNA or *Dlx3* cDNA or VDR gene construct and 1 μg of either pGLuc-vector DNA or pGLuc/*Dlx3* promoter construct with 0.4 μg of pCMV3.1/β-gal were introduced into cells. Then, medium was collected, and cells were harvested 48 h post transfection, and total protein and RNAs were extracted using standard methods for Western blot and real time PCR analyses, respectively. Luciferase activity was determined using *Gaussia* luciferase assay kit (New England Biolabs) and measured using TF2020 Luminometer (Turner Designs) following the manufacturer's instructions. Plasmid pcDNA 3.1 DNA and pGLuc-vector DNA were used as controls, and the relative expression level was normalized against transfection efficiency determined by β-galactosidase activity.

Chromatin Immunoprecipitation—5×10^6 PAM212 cells were transfected with 3 μg of *Hr* cDNA construct and cultured for 48 h. ChIP assays were performed following the protocol provided by the manufacturer (Upstate Biotechnology). Sonicated nuclear extracts were separately incubated with the 2 μg of antibody against either HR (Abfrontier), VDR (Santa Cruz Biotechnology), or normal rabbit IgG (Santa Cruz Biotechnology) overnight at 4 °C. The purified DNA was used for PCR amplification of the *Dlx3* using region-specific primers spanning −613 to −347 bp or −346 to −147 bp or −285 to −1 bp. PCR was performed in 20 μl of reaction mixture containing 1 μl out of 50 μl of the purified DNA with 25 cycles of amplification. Fold enrichment was determined using real time PCR. Primer sequences and PCR conditions were listed in the supplemental Table 1.

Statistical Analysis—*p* values were calculated using the Student's *t* test. $p < 0.05$ values were regarded as statistically significant.

RESULTS

Hairpoor Mice Have Abnormal HF Structure—Previously, we reported abnormal HF morphogenesis in Hr^{Hp}/Hr^{Hp} mice (16). To investigate further the abnormal morphology of Hr^{Hp}/Hr^{Hp} HF, we observed HFs at P7 and P14 using both SEM and

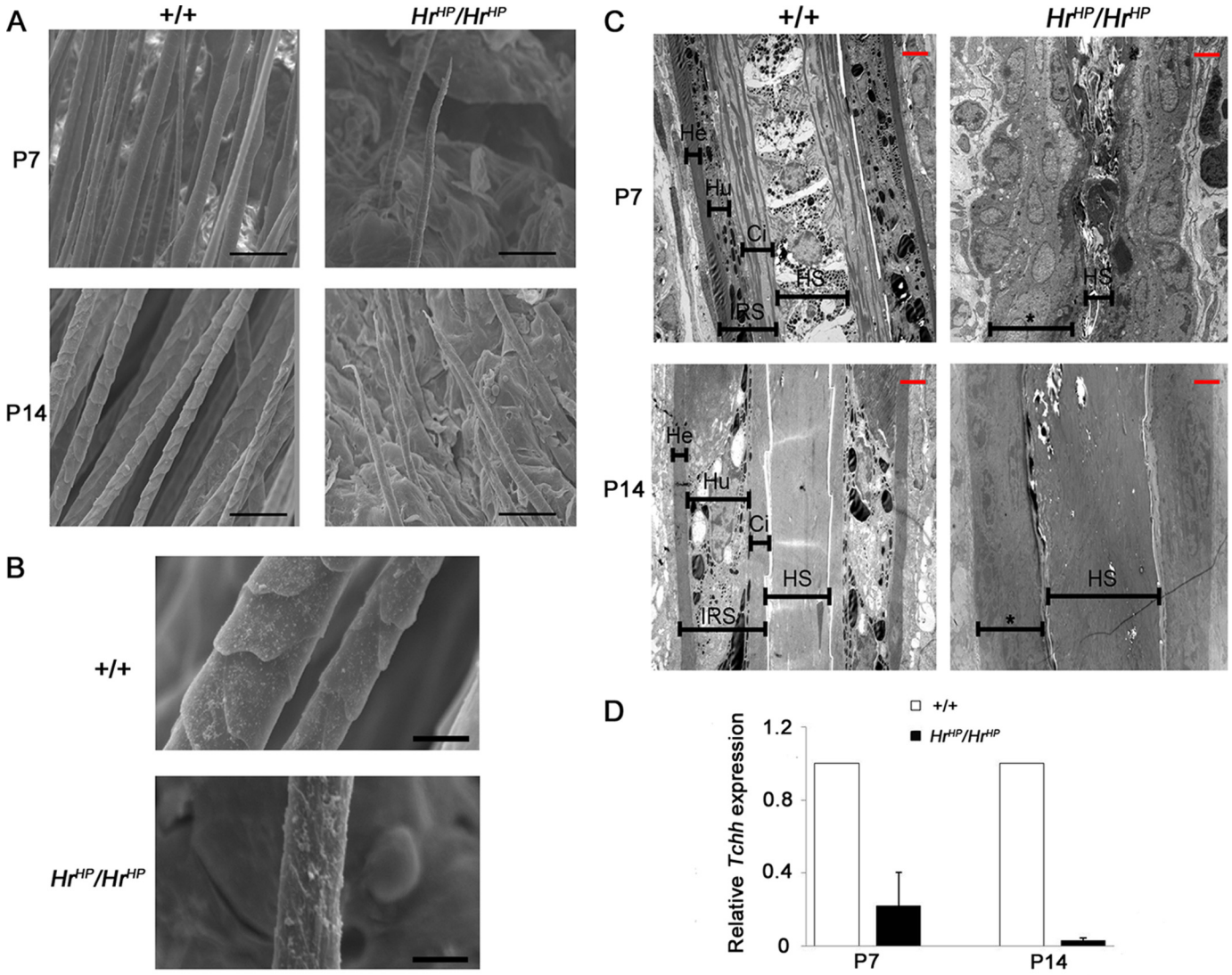

FIGURE 1. **Abnormal formation of the IRS in the Hr^{Hp}/Hr^{Hp} mice.** *A*, SEM images of hair shaft in the wild-type and Hr^{Hp}/Hr^{Hp} mice, at P7 and P14. *Scale bar*, 50 μm. *B*, at P14, Hr^{Hp}/Hr^{Hp} mice had rough hair shaft compared with the wild-type. *Scale bar*, 10 μm. *C*, transmission electron microscopic images of IRS and hair shaft in HFs of the wild-type and Hr^{Hp}/Hr^{Hp} mice, at P7 and P14. *Asterisks* indicate ambiguous structure of IRS. *Scale bar* (*red*) = 2 μm. *He*, Henle's layer; *Hu*, Huxleys's layer; *Ci*, cuticle of IRS. *D*, expression of IRS marker *Tchh* in the wild-type and Hr^{Hp}/Hr^{Hp} mice, at P7 and P14, as determined by real time PCR. The values are the average of the relative expression levels found in three mice, each measured in duplicate (mean ± S.D.).

transmission electron microscopy. SEM analysis revealed the sparse and short hair in Hr^{Hp}/Hr^{Hp} mice at P7 and P14 (Fig. 1*A*). Furthermore, the surface of the hair shaft was very coarse and rough in Hr^{Hp}/Hr^{Hp} mice (Fig. 1*B*). Transmission electron microscopy analysis showed significant disruption of the HF structure in Hr^{Hp}/Hr^{Hp} mice. Wild-type mice displayed a clear boundary of three IRS layers, namely, Henle's, Huxleys's, and cuticle layers, and straight hair shaft at P7. At P14, when hair cycle entered catagen, the three IRS layers were still clearly present in the wild-type mouse. In contrast, prominent alterations of structure within both IRS and hair shaft were observed in Hr^{Hp}/Hr^{Hp} mice. Hr^{Hp}/Hr^{Hp} mice had an ambiguous structure of IRS at both P7 and P14. It was difficult to distinguish the distinct layers of IRS. In addition, the shapes of hair shaft were anomalous with narrow (P7) or extensive shape (P14), compared with those of the wild-type mice (Fig. 1*C*). Because *Hr* was known to express in IRS but not hair shaft, we investigated the expression of trichohyalin (*Tchh*), which were known to express in IRS predominantly at the same time point as for transmission electron microscopy analysis to understand these structural abnormalities in IRS at the molecular level (27). Real time RT-PCR analysis revealed that *Tchh* expression was decreased to 0.22- and 0.03-fold in the Hr^{Hp}/Hr^{Hp} skin at P7 and P14, respectively, compared with that of the age-matched wild-type skin (Fig. 1*D*). These results indicated that *Hr* overexpression mice have abnormal IRS and hair shaft.

Expression of Dlx3 Was Decreased in Hr Overexpressed Mice—The fact that Hr^{Hp}/Hr^{Hp} mice failed to form the normal IRS and HR was a transcriptional co-repressor suggested that deregulation of specific genes expression by overexpressed HR might have caused abnormal formation of IRS in Hr^{Hp}/Hr^{Hp}. In the previous study, we reported many genes whose expressions were affected by *Hr* overexpression (29). Interestingly, the expression of the *Dlx3* mRNA was found to be decreased by 0.45-fold in the Hr^{Hp}/Hr^{Hp} mouse skin compared with that of the wild-type skin at P0 in our microarray analysis (29). Fur-

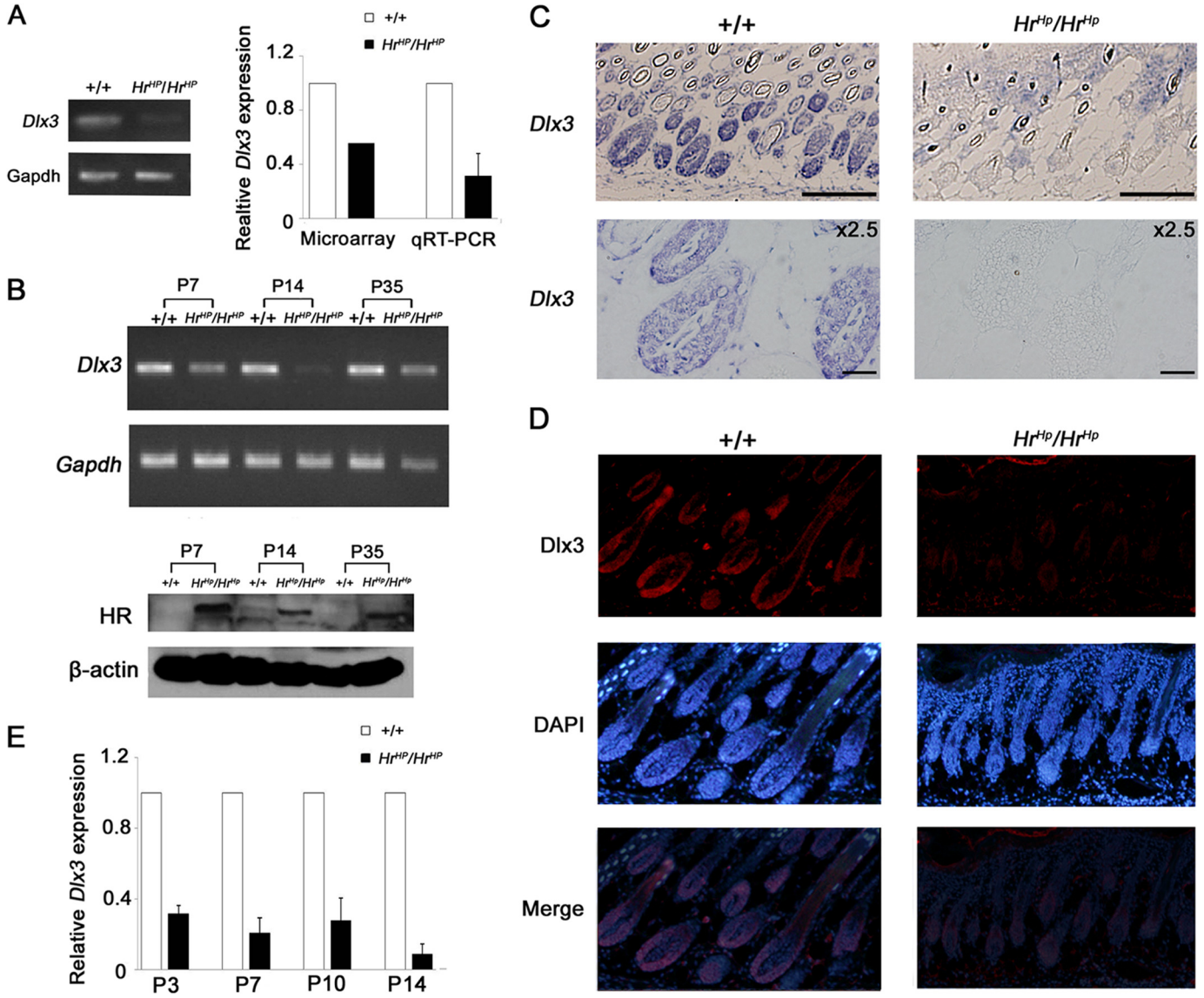

FIGURE 2. **Down-regulation of *Dlx3* in the skin of Hr^{Hp}/Hr^{Hp} mice.** *A*, validation of suppression of *Dlx3* mRNA expression in Hr^{Hp}/Hr^{Hp} skins at P0 by RT-PCR (*left*) and real time PCR (*right*) using the same RNA source as that was used the microarray analysis. *B*, *Dlx3* mRNA expression in the skin of wild-type and Hr^{Hp}/Hr^{Hp} mice, at P7, P14, and P35, as determined by RT-PCR (*top*) HR protein expression in the skin of Hr^{Hp}/Hr^{Hp} mice, at P7, P14, and P35. β-Actin was used as a protein loading control (*bottom*). *C*, *in situ* hybridization of *Dlx3* mRNA in +/+ and Hr^{Hp}/Hr^{Hp} skins at P7. *Scale bar*, 20 μm. *D*, immunohistochemistry of Dlx3 protein (*red*) in the nuclei of +/+ and Hr^{Hp}/Hr^{Hp} skins at P7. DAPI staining (*blue*) indicates nuclei. *E*, down-regulation of *Dlx3* in Hr^{Hp}/Hr^{Hp} skin during HF developmental stages (P0 to P14). The data were normalized against GAPDH mRNA expression. *A* and *E*, the values are the average of the relative expression levels found in three mice, each measured in duplicate (mean ± S.D.).

thermore, *Dlx3* knock-out mice were shown to have a complete hair loss phenotype, which was similar to that of Hr^{Hp}/Hr^{Hp} mice, and *Dlx3* was suggested to play a critical role in HF differentiation and cycling (27).

Based on this information, we hypothesized that *Dlx3* expression was regulated by HR, and HR overexpression caused abnormal HF formation through modulation of *Dlx3* expression in Hr^{Hp}/Hr^{Hp}. To examine our hypothesis, we first validated differential expression of *Dlx3* with mRNAs originally used in the microarray analysis as templates. We observed comparable decrease in *Dlx3* expression in Hr^{Hp}/Hr^{Hp} mouse skin at P0 (Fig. 2*A*). In addition, *Dlx3* expression in Hr^{Hp}/Hr^{Hp} skin was also decreased at P7, P14, and P35 compared with that of the wild-type skin (Fig. 2*B*). Furthermore, *in situ* hybridization and the immunohistochemical staining using *Dlx3*-specific probe and antibody confirmed decreased expression of *Dlx3* mRNA and protein, respectively, in Hr^{Hp}/Hr^{Hp} mouse skin at P7 compared with those of the age-matched wild-type mice (Fig. 2, *C* and *D*, and supplemental Fig. 1). The relative expression level of *Dlx3* mRNA in the Hr^{Hp}/Hr^{Hp} skin was decreased to 0.40- (P0), 0.32- (P3), 0.21- (P7), 0.28- (P10), and 0.04-fold (P14), compared with those of the wild-type skin, as shown by quantitative real time PCR (Fig. 2*E*). Thus, expression of *Dlx3* was decreased continuously in the Hr^{Hp}/Hr^{Hp} skin during the HF morphogenesis.

Whether *Dlx3* expression was regulated by HR in the normal HF development, we also investigated the expression patterns of both *Dlx3* and HR protein in the wild-type mice during hair cycle. Significant HR expression gradually increased from P14 onward, with expression peaking at P21. Then, it was decreased

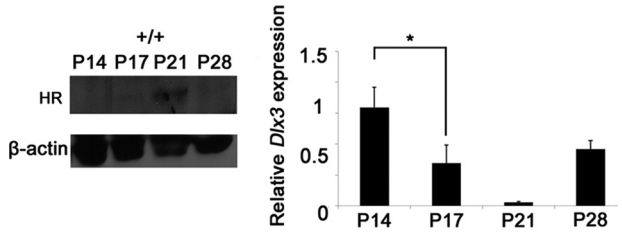

FIGURE 3. **Inverse relationship between *Dlx3* and HR expression in the normal hair cycle.** Western blot showed HR expression in the wild-type skin at P14∼P28 (*left*). *Dlx3* mRNA expression was assessed by quantitative real time PCR in the wild-type skin at P14∼P28 (*right*). The values are the average of the relative expression levels found in three mice, each measured in duplicate (mean ± S.D.). An *asterisk* indicates $p < 0.05$.

at P28, when hair cycle was in new anagen stage (Fig. 3). The real time PCR analysis revealed the inverse relationship between *Dlx3* mRNA expression and the HR expression pattern. *Dlx3* mRNA was highly expressed at P14, which was gradually reduced to 34% and 1.7% at P17 and P21, respectively. At P28, *Dlx3* expression was heightened again to 62% of the expression level at P14 (Fig. 3). These results that *Dlx3* expression showed the inverse relationship to the HR expression in the wild-type skin, and *Dlx3* was down-regulated in the HR overexpressed mouse skin suggested that expression of *Dlx3* may be regulated by HR.

HR Down-regulated Dlx3 Expression in Mouse Keratinocyte—To check the down-regulation of *Dlx3* expression by HR, we examined expression of *Dlx3* using a transient expression system *in vitro*. The relative expression level of *Dlx3* was decreased to 0.36-fold in HR-overexpressed PAM212 mouse keratinocyte, compared with the empty vector transfected control (Fig. 4*A*). This transcriptional suppression of *Dlx3* by HR occurred in a dose-dependent manner as shown by real time PCR analysis (Fig. 4*B*).

To determine the *Dlx3* promoter region responsible for down-regulation by HR, we generated several heterologous reporter constructs by cloning the genomic region of the 5′ flanking sequence of *Dlx3* gene to control expression of the luciferase reporter gene. The 1608-bp DNA fragment showed a promoter activity. Thus, we divided this fragment into three regions (*i.e.* R1, −1608 to −1031 bp; R2, −1064 to −577 bp; and R3, −593 to −1 bp). Although R1 and R2 genomic regions did not show any promoter activity, the R3 genomic region displayed the similar activity as the full-length promoter (Fig. 4*C*). Using R3 and the full-length promoters, the reporter activity was measured and compared in the absence or presence of HR. HR was shown to significantly reduce the promoter activity of both R3 and the full-length promoter by 36 and 26%, respectively (Fig. 4*D*). To determine whether HR binds *Dlx3* promoter, we performed ChIP assay. We divided the R3 fragment into three regions and found that HR specifically binds the region spanning −613 to −286 bp of the *Dlx3* promoter (Fig. 4*E*). From these results, we concluded that HR down-regulates the *Dlx3* expression both *in vivo* and *in vitro* at transcriptional level.

Down-regulation of Dlx3 Expression Resulted in Decrease in IRS Forming Keratin Expression—We previously reported that expression of *Krt71*, a type II IRS keratin, was decreased in Hr^{Hp}/Hr^{Hp} skin and down-regulated by HR overexpression (29). Therefore, we investigated whether HR also regulated expression of type I IRS keratins *Krt25*, *Krt27*, and *Krt28*, the putative heterodimeric partners of *Krt71*. Comparison of expression of these keratin genes between Hr^{Hp}/Hr^{Hp} and wild-type mouse skin revealed that expression of all four keratins was decreased in Hr^{Hp}/Hr^{Hp} skin at P7, P14, and P35 as shown (Fig. 5*A*). Then, we investigated the expression of these genes during HF development (P0 to P14). Although the pattern of suppression was different from each other, we found that expressions of all four keratins were decreased in Hr^{Hp}/Hr^{Hp} skin throughout the HF developmental stages (Fig. 5*A*). To test whether expression of these keratins was dependent on HR, we first investigate the expression of *Krt25*, *Krt27*, *Krt28*, and *Krt71* mRNAs in the PAM212 cells. As shown Fig. 5*B*, we found these IRS keratins expressed in PAM212 cells. Next, we compared expression level of these IRS keratins between the PAM212 cells with control vector transfection and those with *Hr* cDNA construct transfection. In the *Hr* cDNA-transfected cells, the expression of *Krt25*, *Krt27*, *Krt28*, and *Krt71* mRNAs was decreased to 0.60-, 0.58-, 0.32-, and 0.25-fold compared with that of the mock-transfected control, respectively (Fig. 5*C*). However, the basal expression level of *Krt27* was so low that it was difficult to confirm suppression of *Krt27* expression by *Hr*. Nevertheless, these results were basically consistent with their expression pattern *in vivo*, which suggested that HR regulates these IRS-expressing genes.

Because *Dlx3* is reported to control IRS differentiation, we next investigated whether regulation of keratin gene expression by HR was mediated by *Dlx3*. Because we failed to identify any siRNAs capable of inhibition of *Dlx3* expression specifically, we used an overexpression system to determine *Dlx3* effect on keratin expression. As shown in Fig. 5*D*, the expressions of *Krt25*, *Krt27, Krt28*, and *Krt71* were increased in *Dlx3*-overexpressed cells by 3.1-, 4.2-, 2.7-, and 4.2-fold, respectively, compared with those of the mock-transfected cells, whereas *Hr* expression was not affected. This result suggested that Dlx3 indeed positively regulates expression of these keratins. Although it is not clear whether *Krt27* expression was affected by HR and Dlx3 similar to other IRS keratins *in vitro* due to its low basal expression in PAM212 cells (Fig. 5*B*), we cannot exclude the possibility of HR regulation of *Krt27* expression based on *in vivo* results (Fig. 5*A*). Thus, taken together, these findings indicate that HR down-regulates expression of IRS keratins via suppression of *Dlx3* expression.

DISCUSSION

Many genes and signaling pathways, such as the Wnt, Shh, TGFβ/BMP, and FGF, interact with each other and control HF development and cycling (4). The *Hr* gene has been widely studied to delineate its function in hair morphogenesis, as well as in HF cycling. Previous studies showed that HR repressed the expression of Wnt inhibitors, including *Wise*, *Soggy*, *Sfrp1*, and *Sfrp2*, (7, 17, 29, 30), which control Wnt signaling required for HF regeneration.

Using microarray analysis on the skin RNAs, we found that, in addition to the Wnt-associated genes, the expressions of many more genes were regulated by HR (29). Recently, we reported *Foxe1* as a new target of *Hr,* by showing that expres-

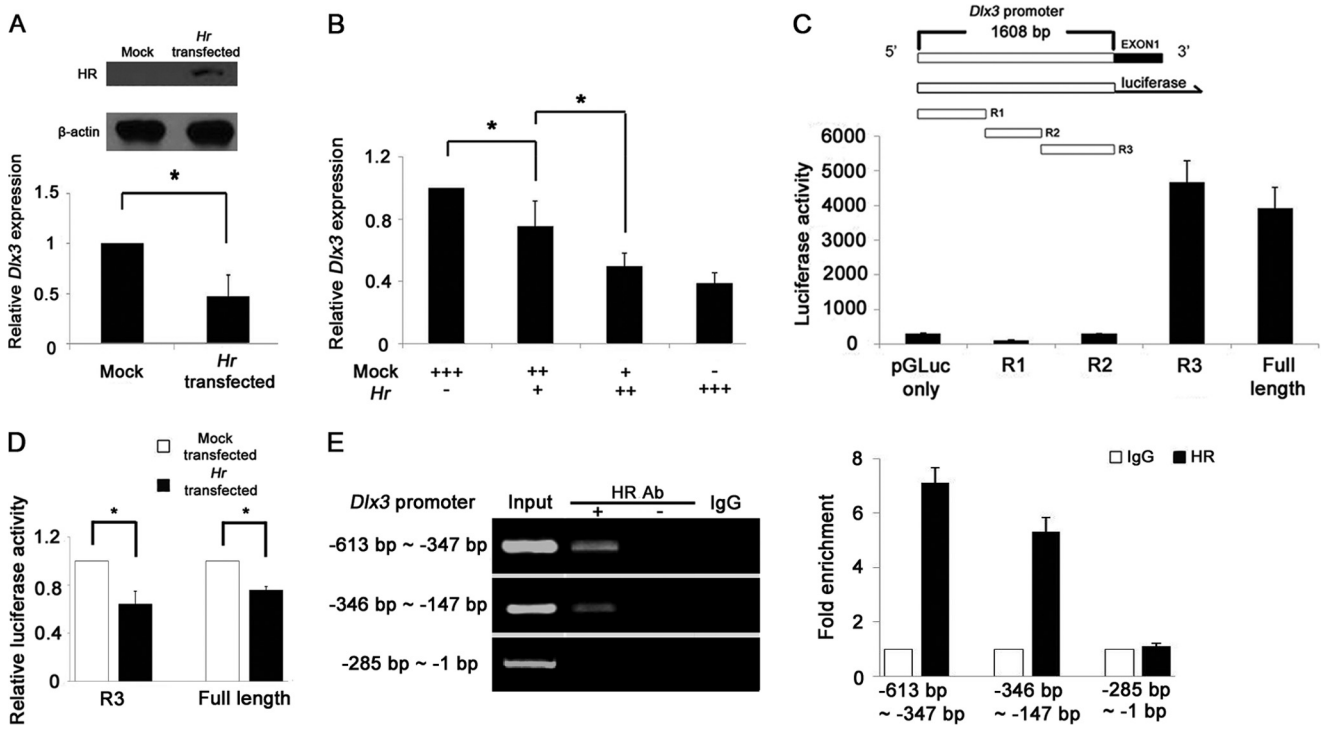

FIGURE 4. **HR down-regulates *Dlx3* mRNA in *Hr*-transfected mouse keratinocyte.** *A*, Western blot analysis showing the HR protein expressed in *Hr*-transfected PAM212 cells. β-Actin indicates equal amount of protein loading (*top*). Down-regulation of *Dlx3* mRNA by HR in *Hr*-transfected PAM212 cells, as determined by real time PCR (*bottom*). *B*, *Dlx3* was down-regulated by HR in a dose-dependent manner. +, 1 μg of DNA used for transfection. *C*, schematic representation of *Dlx3* promoter construct for reporter assay. Promoter activities of the full length (1608 bp), R1, R2, and R3 clones of *Dlx3* were compared with that of the pGLuc-vector. *D*, both R3 and full-length (1608 bp) *Dlx3* promoter activities were decreased by HR expression. The *Dlx3* promoter-fused reporter gene was transfected with the expression vectors of either *Hr* or pcDNA 3.1. Relative luciferase activity was normalized against transfection efficiency determined by β-galactosidase activity. *Asterisks* indicate $p < 0.05$. *A–D*, the activity was the average of three independent experiments conducted in duplicate (mean ± S.D.). *E*, ChIP analyses of HR on *Dlx3* R3 promoters. HR binds the *Dlx3* promoter in the region spanning −613 to −286 bp but not −285 to −1 bp. No antibody and normal IgG were used for the control experiment (*left panel*). Fold enrichment of HR against IgG was quantified using real time PCR performed in duplicate of three repeat experiments (*right panel*).

sion of *Foxe1* was down regulated in Hr^{Hp}/Hr^{Hp} mice (31). *Foxe1* is regulated by the Shh pathway and plays important roles in epithelial-mesenchymal interactions in the HF (32, 33).

In the current study, we added one more HR target gene, *i.e. Dlx3*, a transcription factor that is a target of Wnt pathway and regulates the expression of *Hoxc13* and *Gata3* genes (27). *Dlx3* also controls differentiation of keratinocyte in the hair matrix toward the hair shaft and IRS. Selective ablation of *Dlx3* in mice causes failure in formation of the hair shaft and IRS, leading to complete alopecia (27). These results indicate that *Dlx3* is a crucial regulator of HF differentiation and cycling. Through investigation of the relationship between *Dlx3* and HR, we found the new role of *Hr* in HF formation. Our *in vivo* studies during HF development and *in vitro* observations suggest a role of HR in IRS formation.

IRS forms its structure by obligate heterodimerization of the specified keratins. Type I IRS keratin genes, *i.e. Krt25*, *Krt27*, and *Krt28*, and type II IRS keratin gene *Krt71* are the keratins specifically expressed in all three layers of IRS and known to support the structures of IRS (34, 35). We observed that expression of these IRS keratins was affected consistently by *Hr*, both *in vivo* and *in vitro*. And expression of these genes was dependent on *Dlx3* expression in mouse keratinocyte. Therefore, taken together, these results suggest that, in Hr^{Hp}/Hr^{Hp} skin, down-regulation of *Dlx3* by overexpressed HR causes decrease in expression of the IRS-forming keratins, leading to subsequent abnormal formation of IRS. Decreased IRS keratins may fail to form sufficient amount of heterodimers and therefore cause abnormal formation of IRS. Our data also showed the relationship between HR and *Dlx3* in the hair cycle. In wild-type mice, *Dlx3* was highly expressed at anagen, and its expression began to fall at the beginning of catagen, when HR started to increase in expression. At the peak of HR expression at telogen, *Dlx3* was nearly expressionless (P21, Fig. 3). Further investigation is needed to understand how this reverse relationship between HR and *Dlx3* expression may be related to the cessation of proliferation and the onset of regression of the HF at catagen.

Further study is also required for elucidation of the molecular mechanism of *Dlx3* expression regulated by HR. *Hr* is known as a transcriptional co-repressor, thus suppressing expression of target genes through binding with nuclear receptor transcription factors. Interestingly, none of those transcription factors, which are known to interact with HR have been reported to express in IRS (8, 36–38). Therefore, there are two possibilities. HR may regulate *Dlx3* transcription by directly binding to the region between −613 and −286 bp of the *Dlx3* promoter without interaction with any nuclear receptors. This awaits the further investigation because it has never been documented. A biochemical binding assay with purified HR may resolve the issue.

Alternatively, there may be a transcription factor expressed in IRS yet to be identified, which binds HR and regulates *Dlx3*

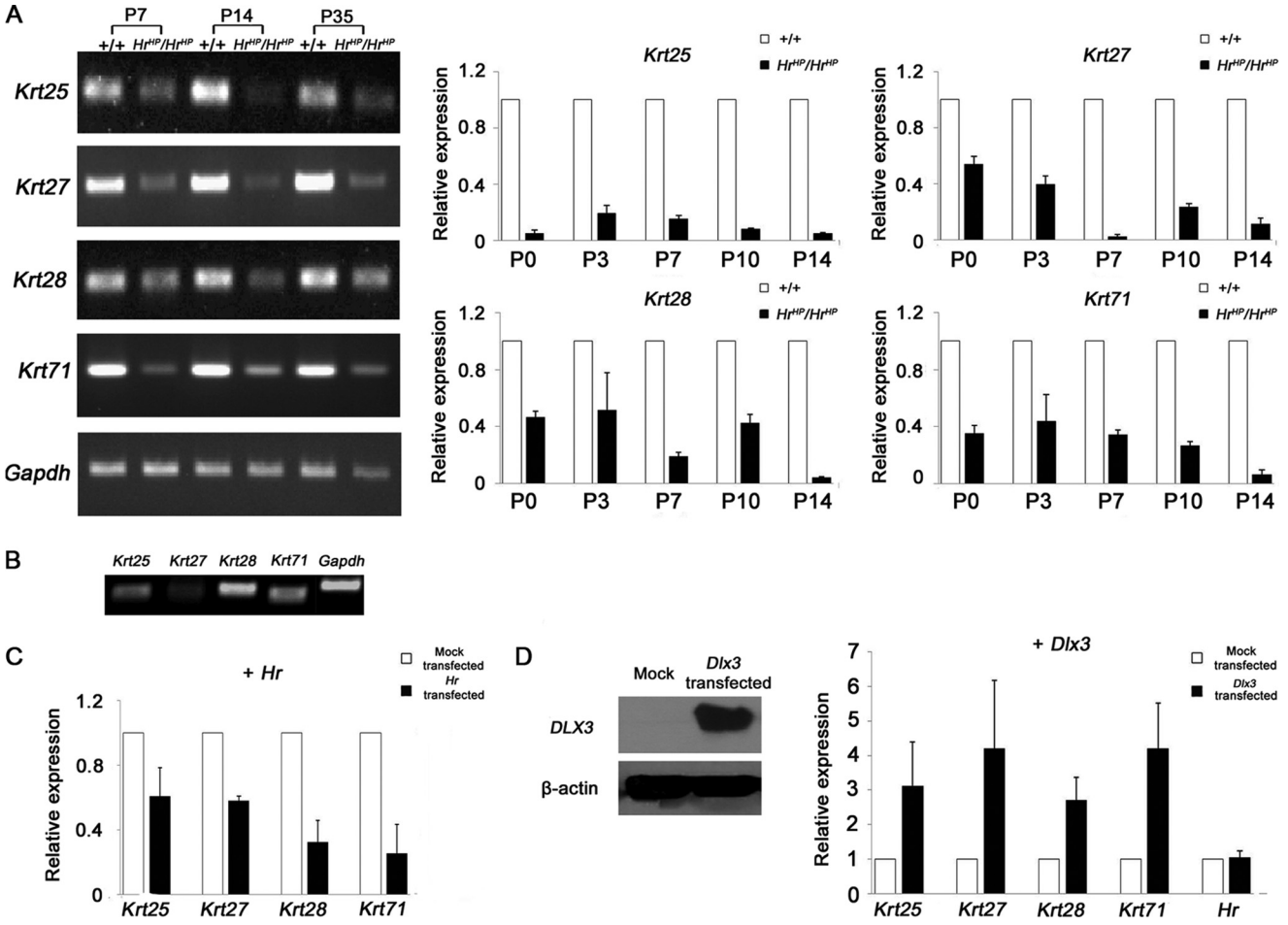

FIGURE 5. **IRS keratin genes, *Krt25*, *Krt27*, *Krt28*, and *Krt71*, were down-regulated in Hr^{Hp}/Hr^{Hp} skins.** *A*, RT-PCR results of *Krt25*, *Krt27*, *Krt28*, and *Krt71* mRNA expression of the wild-type and Hr^{Hp}/Hr^{Hp} skins, at P7, P14, and P35 (*left panel*). Down-regulation of *Krt25*, *Krt27*, *Krt28*, and *Krt71* keratins in the Hr^{Hp}/Hr^{Hp} skin during the HF development stages (P0 to P14). The data were normalized against GAPDH mRNA expression (*right panel*). The values are the average of the relative expression levels determined in three mice, each measured in duplicate (mean ± S.D.). *B*, expression of *Krt25*, *Krt27*, *Krt28*, and *Krt71* in PAM212 cells. *C*, down-regulation of *Krt25*, *Krt27*, *Krt28*, and *Krt71* mRNA by HR in *Hr*-transfected PAM212 cells, as determined by real time PCR (*black bars*). *White bars* indicate the expression of keratins in the cells transfected with pcDNA 3.1 (control). *D*, Western blot analysis showing the Dlx3 protein expressed in PAM212 cells. *β*-Actin indicates equal amount of protein loading (*left*). Up-regulation of *Krt25*, *Krt27*, *Krt28*, and *Krt71* mRNA in *Dlx3*-transfected PAM212 cells, as determined by real time PCR (*right*). pcDNA 3.1 was used as a mock transfection control. *C* and *D*, all of the value is the average of three independent experiments conducted in duplicate (mean ± S.D.).

expression. Through ChIP assay, we found VDR bound the same *Dlx3* promoter region as HR (supplemental Fig. 2), which raised a possibility of VDR mediating regulation of *Dlx3* expression by HR. Indeed, we found that HR further suppressed the *Dlx3* promoter activity in the presence of VDR (supplemental Fig. 3). Thus, HR seems to regulate *Dlx3* expression through VDR and this type of regulation must occur in other HF compartments such as the hair matrix, where HR co-expresses with VDR and *Dlx3*. For example, the abnormal hair shafts in Hr^{Hp}/Hr^{Hp} skin could have been caused by down-regulation of *Dlx3* in the hair matrix where *Hr* and VDR are expressed.

Interestingly, we found that expression of *Hoxc13*, a target of *Dlx3*, which controls hair shaft development, was also down-regulated in Hr^{Hp}/Hr^{Hp} mice as well as in *Hr*-overexpressing mouse keratinocyte (supplemental Fig. 4, *A* and *B*), suggesting a cascade of gene expression for structural formation of the hair shaft. Therefore, overexpressed HR down-regulates several HF-associated transcription factor genes, including *Dlx3* and *Foxe1*, and causes abnormal formation of HF in Hr^{Hp}/Hr^{Hp} mice through cascade of regulation of gene expression (Fig. 6).

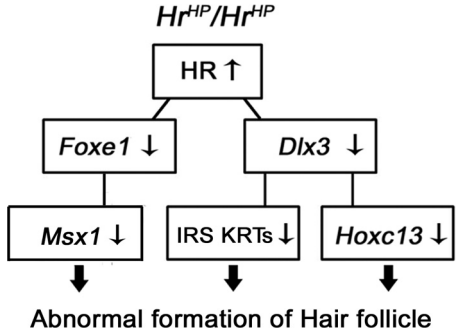

FIGURE 6. **Summary of abnormal HF formation by HR in Hr^{Hp}/Hr^{Hp} mice.** Overexpressed HR down-regulates *Dlx3* and *Foxe1* expression, which mediate subsequent expression regulation of IRS keratins, *Hoxc13* and *Msx1*, resulting in abnormal formation of HF.

In conclusion, our results demonstrate that regulation of *Dlx3* by HR has an important role in the formation of IRS, although further studies are required to delineate the relationship between *Hr* and *Dlx3* in development of HF and regulation of the hair cycle. These studies will provide better understand-

ing for formation of hair follicle and lead to a way for treatment of hair disorders.

REFERENCES

1. Langbein, L., and Schweizer, J. (2005) Keratins of the human hair follicle. *Int. Rev. Cytol.* **243,** 1–78
2. Hardy, M. H. (1992) The secret life of the hair follicle. *Trends Genet.* **8,** 55–61
3. Stenn, K. S., and Paus, R. (2001) Controls of hair follicle cycling. *Physiol. Rev.* **81,** 449–494
4. Krause, K., and Foitzik, K. (2006) Biology of the hair follicle: The basics. *Semin. Cutan. Med. Surg.* **25,** 2–10
5. Panteleyev, A. A., Paus, R., and Christiano, A. M. (2000) Patterns of hairless (hr) gene expression in mouse hair follicle morphogenesis and cycling. *Am. J. Pathol.* **157,** 1071–1079
6. Cachon-Gonzalez, M. B., Fenner, S., Coffin, J. M., Moran, C., Best, S., and Stoye, J. P. (1994) Structure and expression of the hairless gene of mice. *Proc. Natl. Acad. Sci. U.S.A.* **91,** 7717–7721
7. Beaudoin, G. M., 3rd, Sisk, J. M., Coulombe, P. A., and Thompson, C. C. (2005) Hairless triggers reactivation of hair growth by promoting Wnt signaling. *Proc. Natl. Acad. Sci. U.S.A.* **102,** 14653–14658
8. Hsieh, J. C., Sisk, J. M., Jurutka, P. W., Haussler, C. A., Slater, S. A., Haussler, M. R., and Thompson, C. C. (2003) Physical and functional interaction between the vitamin D receptor and hairless corepressor, two proteins required for hair cycling. *J. Biol. Chem.* **278,** 38665–38674
9. Moraitis, A. N., Giguère, V., and Thompson, C. C. (2002) Novel mechanism of nuclear receptor corepressor interaction dictated by activation function 2 helix determinants. *Mol. Cell Biol.* **22,** 6831–6841
10. Thompson, C. C., and Bottcher, M. C. (1997) The product of a thyroid hormone-responsive gene interacts with thyroid hormone receptors. *Proc. Natl. Acad. Sci. U.S.A.* **94,** 8527–8532
11. Zarach, J. M., Beaudoin, G. M., 3rd, Coulombe, P. A., and Thompson, C. C. (2004) The co-repressor hairless has a role in epithelial cell differentiation in the skin. *Development* **131,** 4189–4200
12. Ahmad, W., Panteleyev, A. A., Sundberg, J. P., and Christiano, A. M. (1998) Molecular basis for the rhino (hrrh-8J) phenotype: A nonsense mutation in the mouse hairless gene. *Genomics* **53,** 383–386
13. Mann, S. J. (1971) Hair loss and cyst formation in hairless and rhino mutant mice. *Anat. Rec.* **170,** 485–499
14. Zhang, J. T., Fang, S. G., and Wang, C. Y. (2005) A novel nonsense mutation and polymorphisms in the mouse hairless gene. *J. Invest. Dermatol.* **124,** 1200–1205
15. Liu, Y., Sundberg, J. P., Das, S., Carpenter, D., Cain, K. T., Michaud, E. J., and Voy, B. H. (2010) Molecular basis for hair loss in mice carrying a novel nonsense mutation (Hrrh-R) in the hairless gene (Hr). *Vet. Pathol.* **47,** 167–176
16. Baek, I. C., Kim, J. K., Cho, K. H., Cha, D. S., Cho, J. W., Park, J. K., Song, C. W., and Yoon, S. K. (2009) A novel mutation in Hr causes abnormal hair follicle morphogenesis in hairpoor mouse, an animal model for Marie Unna hereditary hypotrichosis. *Mamm. Genome* **20,** 350–358
17. Kim, J. K., Kim, E., Baek, I. C., Kim, B. K., Cho, A. R., Kim, T. Y., Song, C. W., Seong, J. K., Yoon, J. B., Stenn, K. S., Parimoo, S., and Yoon, S. K. (2010) Overexpression of Hr links excessive induction of Wnt signaling to Marie Unna hereditary hypotrichosis. *Hum. Mol. Genet.* **19,** 445–453
18. Wen, Y., Liu, Y., Xu, Y., Zhao, Y., Hua, R., Wang, K., Sun, M., Li, Y., Yang, S., Zhang, X. J., Kruse, R., Cichon, S., Betz, R. C., Nöthen, M. M., van Steensel, M. A., van Geel, M., Steijlen, P. M., Hohl, D., Huber, M., Dunnill, G. S., Kennedy, C., Messenger, A., Munro, C. S., Terrinoni, A., Hovnanian, A., Bodemer, C., de Prost, Y., Paller, A. S., Irvine, A. D., Sinclair, R., Green, J., Shang, D., Liu, Q., Luo, Y., Jiang, L., Chen, H. D., Lo, W. H., McLean, W. H., He, C. D., and Zhang, X. (2009) Loss-of-function mutations of an inhibitory upstream ORF in the human hairless transcript cause Marie Unna hereditary hypotrichosis. *Nat. Genet.* **41,** 228–233
19. Cohen, S. M., Brönner, G., Küttner, F., Jürgens, G., and Jäckle, H. (1989) Distal-less encodes a homoeodomain protein required for limb development in *Drosophila*. *Nature* **338,** 432–434
20. Feledy, J. A., Morasso, M. I., Jang, S. I., and Sargent, T. D. (1999) Transcriptional activation by the homeodomain protein distal-less 3. *Nucleic Acids Res.* **27,** 764–770
21. Morasso, M. I., Markova, N. G., and Sargent, T. D. (1996) Regulation of epidermal differentiation by a Distal-less homeodomain gene. *J. Cell Biol.* **135,** 1879–1887
22. Morasso, M. I., Grinberg, A., Robinson, G., Sargent, T. D., and Mahon, K. A. (1999) Placental failure in mice lacking the homeobox gene Dlx3. *Proc. Natl. Acad. Sci. U.S.A.* **96,** 162–167
23. Hassan, M. Q., Javed, A., Morasso, M. I., Karlin, J., Montecino, M., van Wijnen, A. J., Stein, G. S., Stein, J. L., and Lian, J. B. (2004) Dlx3 transcriptional regulation of osteoblast differentiation: Temporal recruitment of Msx2, Dlx3, and Dlx5 homeodomain proteins to chromatin of the osteocalcin gene. *Mol. Cell Biol.* **24,** 9248–9261
24. Price, J. A., Bowden, D. W., Wright, J. T., Pettenati, M. J., and Hart, T. C. (1998) Identification of a mutation in DLX3 associated with tricho-dento-osseous (TDO) syndrome. *Hum. Mol. Genet.* **7,** 563–569
25. Price, J. A., Wright, J. T., Kula, K., Bowden, D. W., and Hart, T. C. (1998) A common DLX3 gene mutation is responsible for tricho-dento-osseous syndrome in Virginia and North Carolina families. *J. Med. Genet.* **35,** 825–828
26. Mardaryev, A. N., Ahmed, M. I., Vlahov, N. V., Fessing, M. Y., Gill, J. H., Sharov, A. A., and Botchkareva, N. V. (2010) Micro-RNA-31 controls hair cycle-associated changes in gene expression programs of the skin and hair follicle. *FASEB J.* **24,** 3869–3881
27. Hwang, J., Mehrani, T., Millar, S. E., and Morasso, M. I. (2008) Dlx3 is a crucial regulator of hair follicle differentiation and cycling. *Development* **135,** 3149–3159
28. Nam, Y., Kim, J. K., Cha, D. S., Cho, J. W., Cho, K. H., Yoon, S., Yoon, J. B., Oh, Y. S., Suh, J. G., Han, S. S., Song, C. W., and Yoon, S. K. (2006) A novel missense mutation in the mouse hairless gene causes irreversible hair loss: Genetic and molecular analyses of Hr m1Enu. *Genomics* **87,** 520–526
29. Kim, B. K., Baek, I. C., Lee, H. Y., Kim, J. K., Song, H. H., and Yoon, S. K. (2010) Gene expression profile of the skin in the "hairpoor" (Hr^{Hp}) mice by microarray analysis. *BMC Genomics* **11,** 640
30. Thompson, C. C., Sisk, J. M., and Beaudoin, G. M., 3rd. (2006) Hairless and Wnt signaling: Allies in epithelial stem cell differentiation. *Cell Cycle* **5,** 1913–1917
31. Choi, J. H., Kim, B. K., Kim, J. K., Lee, H. Y., Park, J. K., and Yoon, S. K. (2011) Down-regulation of Foxe1 by HR suppresses Msx1 expression in the hair follicles of Hr(Hp) mice. *BMB Rep.* **44,** 478–483
32. Eichberger, T., Regl, G., Ikram, M. S., Neill, G. W., Philpott, M. P., Aberger, F., and Frischauf, A. M. (2004) FOXE1, a new transcriptional target of GLI2 is expressed in human epidermis and basal cell carcinoma. *J. Invest. Dermatol.* **122,** 1180–1187
33. Brancaccio, A., Minichiello, A., Grachtchouk, M., Antonini, D., Sheng, H., Parlato, R., Dathan, N., Dlugosz, A. A., and Missero, C. (2004) Requirement of the forkhead gene Foxe1, a target of sonic hedgehog signaling, in hair follicle morphogenesis. *Hum. Mol. Genet.* **13,** 2595–2606
34. Tanaka, S., Miura, I., Yoshiki, A., Kato, Y., Yokoyama, H., Shinogi, A., Masuya, H., Wakana, S., Tamura, M., and Shiroishi, T. (2007) Mutations in the helix termination motif of mouse type I IRS keratin genes impair the assembly of keratin intermediate filament. *Genomics* **90,** 703–711
35. Runkel, F., Klaften, M., Koch, K., Böhnert, V., Büssow, H., Fuchs, H., Franz, T., and Hrabé de Angelis, M. (2006) Morphologic and molecular characterization of two novel Krt71 (Krt2–6g) mutations: Krt71rco12 and Krt71rco13. *Mamm. Genome* **17,** 1172–1182
36. Bikle, D. D., Elalieh, H., Chang, S., Xie, Z., and Sundberg, J. P. (2006) Development and progression of alopecia in the vitamin D receptor null mouse. *J. Cell Physiol.* **207,** 340–353
37. Billoni, N., Buan, B., Gautier, B., Gaillard, O., Mahé, Y. F., and Bernard, B. A. (2000) Thyroid hormone receptor β1 is expressed in the human hair follicle. *Br. J. Dermatol.* **142,** 645–652
38. Steinmayr, M., André, E., Conquet, F., Rondi-Reig, L., Delhaye-Bouchaud, N., Auclair, N., Daniel, H., Crépel, F., Mariani, J., Sotelo, C., and Becker-André, M. (1998) Staggerer phenotype in retinoid-related orphan receptor α-deficient mice. *Proc. Natl. Acad. Sci. U.S.A.* **95,** 3960–3965